Int. J. Solids Structures, 1972, Vol. 8, pp. 627 to 650. Pergamon Press. Printed in Great Britain

ON WAVE PROPAGATION AND ENERGY SCATTERING IN MATERIALS REINFORCED BY INEXTENSIBLE FIBERS†

YECHIEL WEITSMAN‡

School of Engineering, Tel-Aviv University, Tel-Aviv, Israel

Abstract—This paper concerns the propagation of elastic waves in materials reinforced by inextensible fibers. Slowness surfaces, energy fluxes and directions of propagation are determined and expressed in terms of material properties and fiber directions.

The case of two domains of fiber-reinforced materials, similar in all respects except for fiber direction, and bonded together at a plane interface, is considered in detail. The misalignment in fiber directions that occurs at the bonded interface is shown to cause a significant scattering of mechanical energy.

The range of validity of the mathematical model employed in this paper is indicated and it is shown that the results may be useful in practical cases.

The existance of surface waves is also discussed.

INTRODUCTION

MANY investigations concerning the mechanical behavior of composite materials, mostly regarding their static response, were conducted in recent years. A survey of the significant contributions up to the mid sixties was given by Hashin [1]. Another detailed exposition concerning the static analysis of fiber-reinforced materials was published recently [2].

The major aim, of most of the theoretical investigations concerning composite materials, was the establishment of constitutive equations which describe the mechanical response of a multi-phase medium in a mathematically tractable manner. This aim was practically achieved by means of the "effective modulus theory". The "effective modulus theory" represents approximately the static response of a multi-phase medium by the behavior of an equivalent homogeneous material. The approximation is accomplished by deriving the "best" equivalent moduli for the representative homogeneous material, so that it reproduces the mechanical response of the composite in some average sense.

In the case of a fiber-reinforced matrix, the composite can be approximated by a homogeneous, transversely isotropic material [2]. In this case the approximation yields expressions for the five "equivalent moduli" of the transversely isotropic medium.

The dynamic behavior of composite materials is much more intricate than their static response. The major added complication is due to the many reflections and refractions of waves, that occur within the composite material, at the inner boundaries between the various material constituents. These dynamic interactions at the inner interfaces give rise to wave dispersion, a phenomenon which is ignored by the "effective modulus theory".

Some aspects of wave propagation in orderly layered, or laminated, composites were analyzed and solved exactly [3, 4]. In those cases expressions were given for "effective

† This work was supported by Contract No. DAJA37-71-C-1579.

‡ Associate Professor, Department of Engineering Sciences, Tel-Aviv University, Ramat-Aviv, Tel-Aviv, Israel.

moduli" as relevant for each particular problem. It has been shown that for laminated media the effective modulus theory yielded results which were in reasonably good agreement with the exact solution for waves of large wave length.

No exact solution is available at present for a wave propagation problems in fiber-reinforced materials. In the absence of any reliable basis for comparison it is conjectured that the effective modulus theory can be employed to predict the dynamic behavior of fiber-reinforced composites, provided that the one recognizes that the validity of the conclusions is restricted to the large wave length range.

This paper considers some aspects of wave propagation in elastic materials reinforced with inextensible fibers. In a forthcoming work [5], it will be proven that the theory of materials reinforced by inextensible cords is essentially an "equivalent modulus" formulation.

As has been already stated, the range of validity of the results presented herein is clearly restricted to waves of long wave length and low frequency. The results fail to incorporate the dispersion that is caused by the intra-phase boundaries.

On the other hand this paper illuminates the dispersive effects of misalignments in fiber directions.

A fiber-reinforced material is endowed by the fibers with a preferred direction. Various wave quantities are related to, and determined by, the directions of the fibers. If, for instance, two semi-infinite fiber-reinforced material regions, which are similar in all respects but differ in the fiber directions, are bonded together at a plane boundary, then a most significant diffraction of waves may occur at the interface even at low frequencies and for long wave lengths.

This aspect, of diffraction of waves due to fiber misalignment, has not been investigated thus far.

The mathematical method employed in this work is based upon the classical formulation of wave propagation in anisotropic materials [6, 7]. In spite of its limitations, this mathematical model has the significant advantage of simplicity. Due to this simplicity of the model it was possible to investigate analytically a phenomenon that is much too cumbersome to analyze otherwise.

For the sake of completeness, this paper includes a discussion of surface waves in elastic materials reinforced with rigid fibers. It is shown that under special circumstances it is possible to recover the Rayleigh wave.

BASIC CONSIDERATIONS

Consider a material body reinforced by a very large number of inextensible fibers. Let the distances between adjacent fibers be much smaller than the dimensions of the body, assume all the fibers to be parallel to a common direction $\mathbf{n}$ ($|\mathbf{n}| = 1$). In general $\mathbf{n}$ may vary in space, so that $\mathbf{n} = \mathbf{n}(\mathbf{x})$. In this paper the standard index notation will be employed, e.g. $\mathbf{x} = x_i\mathbf{e}_i = x_1\mathbf{e}_1 + x_2\mathbf{e}_2 + x_3\mathbf{e}_3$.

Assume that the fibers extend without interruption from one end of the body to the other. In view of their close spacing and inextensibility the fibers impose on the material the geometric constraint

$$\varepsilon_{nn}(\mathbf{x}) = 0 \tag{1}$$

where ε_{nn} is the component of strain in the direction of $\mathbf{n}$.

Denote by U the strain-energy density of an isotropic body. In the linear elastic case we have

$$U = \tfrac{1}{2}\lambda\varepsilon_{ii}\varepsilon_{jj} + \mu\varepsilon_{ij}\varepsilon_{ij} \tag{2}$$

where λ and μ are the Lamé constants.

In general, the components of the stress tensor σ_{ij} are taken as the derivatives of U with respect to the corresponding components of the strain ε_{ij}. However in the present case, the components of ε_{ij} are not all independent, because of the geometrical constraint (1) which requires that

$$\varepsilon_{nn} = \varepsilon_{pq}n_p n_q = 0. \tag{3}$$

Employing a Lagrange multiplier τ we write

$$\sigma_{ij} = \frac{\partial}{\partial\varepsilon_{ij}}(\tfrac{1}{2}\lambda\varepsilon_{rr}\varepsilon_{ss} + \mu\varepsilon_{rs}\varepsilon_{rs} + \tau\varepsilon_{pq}n_p n_q) \tag{4}$$

whence we obtain

$$\sigma_{ij} = \lambda\varepsilon_{kk}\delta_{ij} + 2\mu\varepsilon_{ij} + \tau n_i n_j. \tag{5}$$

The quantity τ expresses an indeterminate tension in the direction of the fibers. This quantity cannot be determined from the constitutive equations and is only decided in terms of imposed traction boundary conditions.

Equation (5) is a linearized version of the nonlinear theory of elastic materials reinforced by inextensible cords [8].

As already noted it is possible to represent a fiber-reinforced composite body by a homogeneous transversely isotropic body [2]. In general, the constitutive relation for transverse isotropy about a direction **n** reads [9]:

$$\sigma_{ij} = \lambda\varepsilon_{kk}\delta_{ij} + 2\mu\varepsilon_{ij} + \alpha(\varepsilon_{\mathbf{nn}}\delta_{ij} + n_i n_j\varepsilon_{kk}) + 2\beta(\varepsilon_{ik}n_j n_k + \varepsilon_{jk}n_i n_k) + \gamma\varepsilon_{\mathbf{nn}}n_i n_j. \tag{6}$$

In (6) the quantity $\varepsilon_{\mathbf{nn}}$ is the strain in the direction of **n**.

Equation (5) represents a limiting case of (6), with $\alpha = \beta = 0$ and when $\varepsilon_{\mathbf{nn}} = 0$ but $\gamma \to \infty$ so that $\gamma\varepsilon_{\mathbf{nn}} = \tau$.

In order to appreciate the physical meaning of the limit $\gamma \to \infty$ and $\alpha = \beta = 0$ it is necessary to perform some detailed and cumbersome calculations, converting the quantities $\lambda, \mu, \alpha, \beta, \gamma$ which appear in equation (6) to the moduli employed in Ref. [2]. For the sake of brevity these calculations will be given elsewhere [5].

At present, the conclusions will be stated without proof. Accordingly, the model of an elastic material reinforced by inextensible cords provides a useful tool for studying wave propagation phenomena in a fiber-reinforced matrix under the following circumstances:

1. The fibers are much more rigid than the matrix.
2. A small volume fraction of fiber material.
3. The distances between adjacent fibers are much smaller than the dimensions of the body.
4. The Poisson's ratio of the matrix material is close to zero.†
5. The wave lengths considered are much larger than intra-fiber distances.

† For small volume fractions of fiber material the approximation remains valid for any value of Poisson's ratio of the fibers.

SLOWNESS SURFACES FOR EXTENSIBLE FIBERS

Consider first the constitutive equation (6) with $\alpha = \beta = 0$ but with finite γ.

Let ω be the frequency of a harmonic wave and $\mathbf{s}$ its slowness vector [6, 7]. Let the displacement components be given by

$$u_j = Ap_j e^{i\omega(\mathbf{s}.\mathbf{x}-t)}. \tag{7}$$

In (7) A is the amplitude, $\mathbf{p}$ is a unit vector in the direction of $\mathbf{u}$ and t denotes time.

With $\alpha = \beta = 0$ in (6), the dynamic equations $\sigma_{ij,j} = \rho\ddot{u}_i$ read

$$[(\lambda+\mu)s_is_k + \mu s_js_j\delta_{ik} + \gamma(n_js_j)^2n_in_k]p_k = p_i \tag{8}$$

or

$$(\rho-\mu s^2)\mathbf{p} = (\lambda+\mu)(\mathbf{s}\,.\,\mathbf{p})\mathbf{s} + \gamma(\mathbf{n}\,.\,\mathbf{s})^2(\mathbf{n}\,.\,\mathbf{p})\mathbf{n}. \tag{9}$$

In order to solve (9) consider the following

(a) $s^2 = \rho/\mu = c_2^{-2}$, where c_2 is the velocity of propagation of shear waves. In this case we must have $\mathbf{s}\,.\,\mathbf{p} = 0$ and $\mathbf{n}\,.\,\mathbf{p} = 0$.

This means that one slowness surface is a sphere of radius $1/c_2$. If $\mathbf{n}$, the fiber direction, coincides with the polar axis of this sphere, then the displacement $\mathbf{p}$ is always parallel to the latitudinal directions.

There are however, two exceptions:

(i) $\mathbf{n}\,.\,\mathbf{s} = 0, \mathbf{s}\,.\,\mathbf{p} = 0$

which means that on the equator of the above mentioned sphere there exist also displacements $\mathbf{p}$ in the direction of $\mathbf{n}$.

(ii) $\mathbf{s}\|\mathbf{n}$

which, in view of (9) yields

$$(\lambda+\mu+\gamma)\mathbf{n}\,.\,\mathbf{p} = 0 \qquad \text{i.e. } \mathbf{n}\,.\,\mathbf{p} = 0.$$

This means that at the poles there exist displacements in all directions tangent to the sphere.

(b) $s^2 \neq \rho/\mu$. In this case

$$\mathbf{p} = a\mathbf{s} + b\mathbf{n}.$$

From (9) we obtain

$$(1-c_2^2s^2)(a\mathbf{s}+b\mathbf{n}) = (c_1^2-c_2^2)[as^2 + b(\mathbf{n}\,.\,\mathbf{s})]\mathbf{s} + \frac{\gamma}{\rho}(\mathbf{n}\,.\,\mathbf{s})^2[a(\mathbf{n}\,.\,\mathbf{s})+b]\mathbf{n}.$$

In the above equation $c_1^2 = (\lambda+2\mu)/\rho$.

We get

$$\begin{aligned}(1-c_2^2s^2)a &= (c_1^2-c_2^2)s^2a + (c_1^2-c_2^2)(\mathbf{n}\,.\,\mathbf{s})b\\ (1-c_2^2s^2)b &= \frac{\gamma}{\rho}(\mathbf{n}\,.\,\mathbf{s})^3a + \frac{\gamma}{\rho}(\mathbf{n}\,.\,\mathbf{s})^2b.\end{aligned} \tag{10}$$

Let θ be the angle between $\mathbf{n}$ and $\mathbf{s}$, then $\mathbf{n}\,.\,\mathbf{s} = s\cos\theta = s_n$. From the determinant of (10) we get

$$\frac{\gamma}{\rho}(c_1^2-c_2^2)s_n^4 + \frac{\gamma}{\rho}(1-c_1^2s^2)s_n^2 - (1-c_1^2s^2)(1-c_2^2s^2) = 0 \tag{11}$$

therefore

$$s_n^2 = \frac{\rho}{2\gamma(c_1^2-c_2^2)}\left\{-\frac{\gamma}{\rho}(1-c_1^2s^2)\left[\pm\left(\frac{\gamma}{\rho}\right)^2(1-c_1^2s^2)^2+4\frac{\gamma}{\rho}(c_1^2-c_2^2)(1-c_1^2s^2)(1-c_2^2s^2)\right]^{\frac{1}{2}}\right\}.$$

For $\mathbf{s}\perp\mathbf{n}$, $s_n = 0$ and (11) yields

$$s^2 = c_1^{-2} \qquad \text{or} \qquad s^2 = c_2^{-2}.$$

For $\mathbf{s}\parallel\mathbf{n}$, $\mathbf{s}_n = s$ so that we obtain

$$c_2^2\left(c_1^2+\frac{\gamma}{\rho}\right)s^4-\left(c_2^2+c_1^2+\frac{\gamma}{\rho}\right)s^2+1 = 0$$

whence

$$s^2 = c_2^{-2} \qquad \text{or} \qquad s^2 = \left(c_1^2+\frac{\gamma}{\rho}\right)^{-1}.$$

For small values of γ the slowness surfaces are sketched in Fig. 1. In the isotropic case, $\gamma = 0$, the slowness surfaces are two spheres $|\mathbf{s}| = c_1^{-1}$, $|\mathbf{s}| = c_2^{-1}$.

Now, an alternative form of (11) is

$$\left[\frac{\gamma}{\rho}(c_1^2-c_2^2)\cos^4\theta-\frac{\gamma}{\rho}c_1^2\cos^2\theta-c_1^2c_2^2\right]s^4+\left(\frac{\gamma}{\rho}\cos^2\theta+c_1^2+c_2^2\right)s^2-1 = 0$$

or

$$\left[\frac{\gamma}{\rho}\cos^2\theta(c_2^2\cos^2\theta+c_1^2\sin^2\theta)+c_1^2c_2^2\right]s^4-\left(\frac{\gamma}{\rho}\cos^2\theta+c_1^2+c_2^2\right)s^2+1 = 0. \tag{12}$$

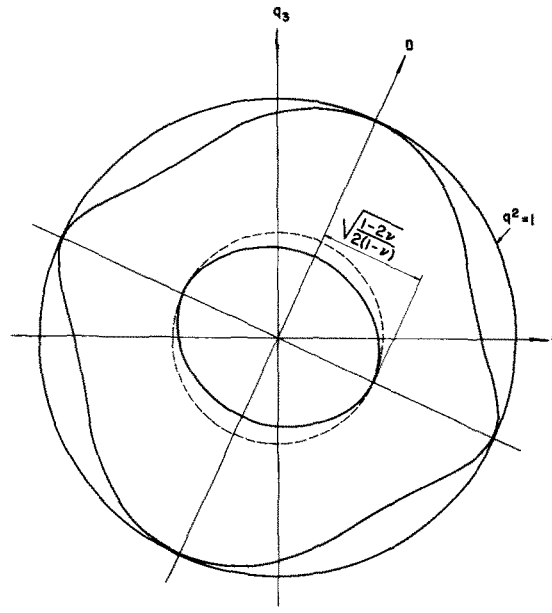

FIG. 1. A sketch of the slowness surfaces for small γ.

For large γ, (12) yields

$$(c_2^2 \cos^2\theta + c_1^2 \sin^2\theta)s^4 - s^2 = 0$$

therefore

$$s^2 = (c_2^2 \cos^2\theta + c_1^2 \sin^2\theta)^{-1} \qquad \text{or} \qquad s \to 0. \tag{13}$$

For small s a more precise conclusion from (12) is

$$s^2 = \frac{\rho}{\gamma \cos^2\theta}. \tag{14}$$

If γ is large but $\cos^2\theta \to 0$ so that $\gamma \cos^2\theta$ remains finite, then, by (12)

$$\left(\frac{\gamma}{\rho}\cos^2\theta c_1^2 + c_1^2 c_2^2\right)s^4 - \left(\frac{\gamma}{\rho}\cos^2\theta + c_1^2 + c_2^2\right)s^2 + 1 = 0.$$

In this case we conclude that

$$s^2 = c_1^{-2}$$

and (15)

$$s^2 = \left(\frac{\gamma}{\rho}\cos^2\theta + c_2^2\right)^{-1}.$$

The second of (15) is equivalent to

$$\frac{\gamma}{\rho}s_n^2 + c_2^2 s^2 = 1.$$

Finally, an additional feature of the slowness surfaces for large γ and small values of $\cos\theta$ is obtained by rewriting (11) as follows

$$(1 - c_1^2 s^2)\left(\frac{\gamma}{\rho}s_n^2 + c_2^2 s^2 - 1\right) = -\frac{\gamma}{\rho}(c_1^2 - c_2^2)s_n^4$$

whereby

$$\frac{\gamma}{\rho}s_n^2 + c_2^2 s^2 = 1 + \frac{\gamma}{\rho}(c_1^2 - c_2^2)\frac{s_n^4}{c_1^2 s^2 - 1}. \tag{16}$$

It may be seen from (16) that as $c_1 s \to 1^+$ the radius of the slowness surface increases, while as $c_1 s \to 1^-$ the corresponding radius decreases.

Finally, by solving for the ratio of $a : b$ in equation (10) we have from $\mathbf{p} = a\mathbf{s} + b\mathbf{n}$ that the displacement $\mathbf{u}$ is proportional to

$$\mathbf{u} = (c_1^2 - c_2^2)s_n\mathbf{s} + (1 - c_1^2 s^2)\mathbf{n}. \tag{17}$$

Slowness surfaces for large values of γ are sketched in Fig. 2.

SLOWNESS SURFACES FOR RIGID FIBERS

Consider now the limiting case of rigid fibers as represented in equation (5). Let

$$\mathbf{u} = A\mathbf{p}\, e^{i\omega(\mathbf{s}\cdot\mathbf{x} - t)}$$

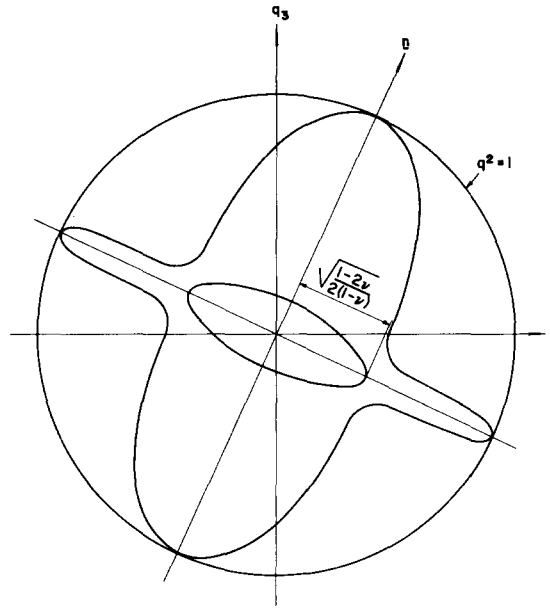

FIG. 2. A sketch of the slowness surfaces for large γ.

and the arbitrary reaction τ be

$$\tau = i\omega T\, e^{i\omega(\mathbf{s}.\mathbf{x}-t)}.$$

The equations of motion for the constitutive equation (5) read

$$(\rho-\mu s^2)\mathbf{p} = (\lambda+\mu)(\mathbf{s}\,.\,\mathbf{p})\mathbf{s}+T(\mathbf{n}\,.\,\mathbf{s})\mathbf{n}. \tag{18}$$

In addition, the constraint $\varepsilon_{\mathbf{nn}} = 0$, i.e. $u_{i,j}n_in_j = 0$, yields

$$(\mathbf{p}\,.\,\mathbf{n})(\mathbf{s}\,.\,\mathbf{n}) = 0. \tag{19}$$

In view of (19) there exist two cases:

(a) $\mathbf{s}\,.\,\mathbf{n} = 0$. Then

(i) $s^2 = \rho/\mu = c_2^{-2}$ and $\mathbf{s}\,.\,\mathbf{p} = 0$ or (20)

(ii) $s^2 = \rho/(\lambda+2\mu) = c_1^{-2}$

and $\mathbf{p} \parallel \mathbf{s}$.

(b) $\mathbf{p}\,.\,\mathbf{n} = 0$. Then, by (18)

$$T(\mathbf{n}\,.\,\mathbf{s})+(\lambda+\mu)(\mathbf{s}\,.\,\mathbf{p})(\mathbf{s}\,.\,\mathbf{n}) = 0 \tag{21}$$

whereby

$$(\rho-\mu s^2)\mathbf{p} = (\lambda+\mu)(\mathbf{s}\,.\,\mathbf{p})[\mathbf{s}-(\mathbf{s}\,.\,\mathbf{n})\mathbf{n}]. \tag{22}$$

In this case there exist two possibilities:

$$\text{(i)}\quad s^2 = \rho/\mu = c_2^{-2} \tag{23}$$

and

$$\mathbf{p}\,.\,\mathbf{s} = 0.$$

(ii) **p** parallel to $\mathbf{s}-(\mathbf{s}\,.\,\mathbf{n})\mathbf{n}$ which yields

$$\rho-\mu s^2 = (\lambda+\mu)(s^2-s_n^2). \tag{24}$$

Equation (22) can be rewritten to read

$$(c_1^2\sin^2\theta+c_2^2\cos^2\theta)s^2 = 1$$

showing that this equation describes an ellipsoid of revolution about the axis of **n**.

In the subsequent analysis it was found advantageous to introduce the non-dimensional slowness $\mathbf{q} = c_2\mathbf{s}$. In terms of **q**, equation (23) describes the sphere $|\mathbf{q}| = 1$, while the ellipsoid (24) is given by

$$2\frac{1-\nu}{1-2\nu}q^2-\frac{1}{1-2\nu}(\mathbf{q}\,.\,\mathbf{n})^2 = 1. \tag{25}$$

In addition, we have slownesses lying on the equatorial circle as described by equation (20).

The spherical and ellipsoidal slowness surfaces, and the equatorial "slowness circle", are shown in Fig. 3.

An inspection of Figs. 2 and 3 indicates that the ellipsoid and the equatorial ring are traces of two interior slowness surfaces that exist for finite values of γ. The horizontal portions of the interior slowness surfaces disappear when $\gamma \to \infty$. It will be seen later that their disappearance is compensated by the presence of arbitrary reactions in direction **n**.

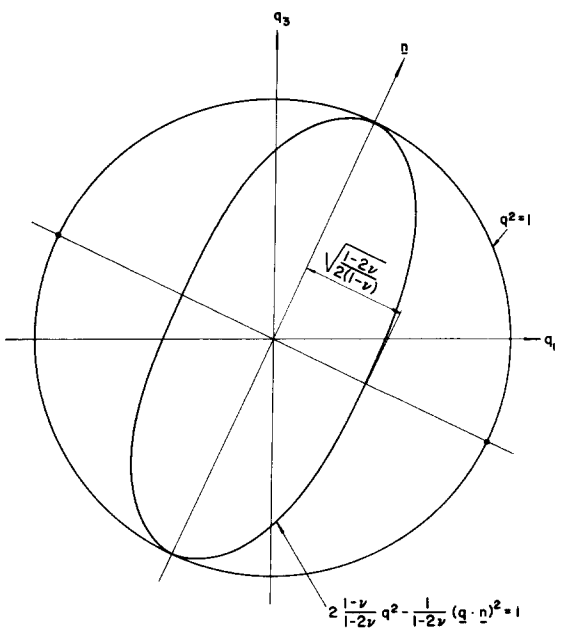

FIG. 3. A sketch of the slowness surfaces for rigid fibers.

STRESS AND DISPLACEMENT FIELDS IN THE CASE OF RIGID FIBERS

1. *Consider* $\mathbf{p} \cdot \mathbf{n} = 0$

In view of (21) we have

$$\sigma_{ij} = A\{[\lambda\delta_{ij} - (\lambda+\mu)n_i n_j]s_k p_k + \mu(p_i s_j + p_j s_i)\} i\omega \, e^{i\omega(\mathbf{s}.\mathbf{x}-t)} \tag{26}$$

and, from (22),

$$\{(\lambda+\mu)[s_i s_k - s_j n_j n_i s_k] + (\mu s^2 - \rho)\delta_{ik}\} p_k = 0. \tag{27}$$

Setting the determinant of (27) to be zero, we obtain

$$(\mu s^2 - \rho)^2\{\mu s^2 - \rho + (\lambda+\mu)[s^2 - (\mathbf{s} \cdot \mathbf{n})^2]\} = 0.$$

(i) Consider $\mu s^2 - \rho = 0$, namely the slowness surface $|\mathbf{q}| = 1$. In this case equation (27) yields $\mathbf{p} \cdot \mathbf{q} = 0$. Together with $\mathbf{p} \cdot \mathbf{n}$ we obtain

$$\mathbf{p} = \mathbf{n} \times \mathbf{q}/|\mathbf{n} \times \mathbf{q}|. \tag{28}$$

Therefore the spherical slowness surface is associated with shear waves whose displacements are in directions transverse to $\mathbf{n}$ as sketched in Fig. 4. This wave will be denoted the "transverse shear" $(T-S)$ wave.

With $\mathbf{p} \cdot \mathbf{q} = 0$ equation (26) yields

$$\sigma_{ij} = A\mu(p_i s_j + p_j s_i) i\omega \, e^{i\omega(\mathbf{s}.\mathbf{x}-t)}. \tag{29}$$

For the sake of brevity terms like $i\omega \, e^{i\omega(\mathbf{s}.\mathbf{x}-t)}$ will be omitted in the remainder of this paper.

A substantial simplification is achieved in the formulation if q_2 is taken to be zero. This can be done without loss of generality because the slowness surfaces are bodies of

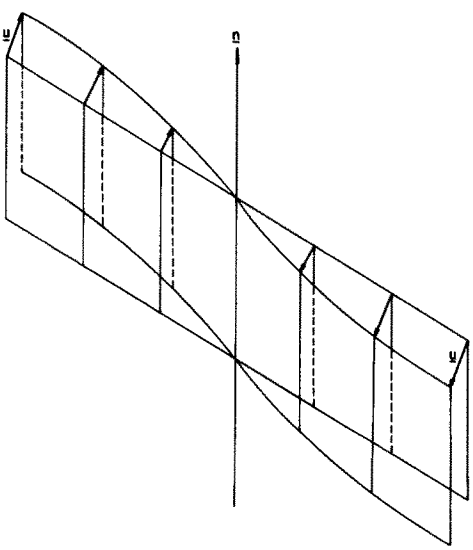

FIG. 4. Displacements corresponding to the T–S waves.

revolution about the axis of **n**. With this additional simplification we have for the T–S wave:

$$u_1 = Kn_2q_3 \tag{30.1}$$

$$u_2 = K(n_3q_1 - n_1q_3) \tag{30.2}$$

$$u_3 = -Kn_2q_1 \tag{30.3}$$

$$\sigma_{31} = \bar{K}n_2(q_3^2 - q_1^2) \tag{30.4}$$

$$\sigma_{32} = \bar{K}(n_3q_1 - n_1q_3)q_3 \tag{30.5}$$

$$\sigma_{33} = -2\bar{K}n_2q_1q_3. \tag{30.6}$$

In (30) $K = (A/|\mathbf{n}\times\mathbf{q}|)\,e^{i\omega(\mathbf{s}.\mathbf{x}-t)}$, $\bar{K} = i\omega(\mu/c_2)K$ and $q_3^2 = 1 - q_1^2$.

(ii) Consider now

$$\mu s^2 + (\lambda+\mu)[s^2 - (\mathbf{s}\,.\,\mathbf{n})^2] - \rho = 0. \tag{31}$$

Equation (31) is equivalent to (25) and represents the ellipsoidal surface. In this case equation (27) yields, after several straightforward manipulations,

$$\mathbf{p} = (\mathbf{n}\times\mathbf{q})\times\mathbf{n}/|\mathbf{n}\times\mathbf{q}|. \tag{32}$$

This displacement is normal to the polar axis **n** and directed towards it. Therefore, the wave has the character of a "normal compression" wave. It will be denoted by $N-C$ (Fig. 5).

In view of (32) it follows that

$$s_kp_k = (1/|\mathbf{n}\times\mathbf{s}|)[s^2 - (\mathbf{s}\,.\,\mathbf{n})^2]$$

whereby, together with (31), we get

$$(\lambda+\mu)s_kp_k = (1/|\mathbf{n}\times\mathbf{s}|)(\rho - \mu s^2). \tag{33}$$

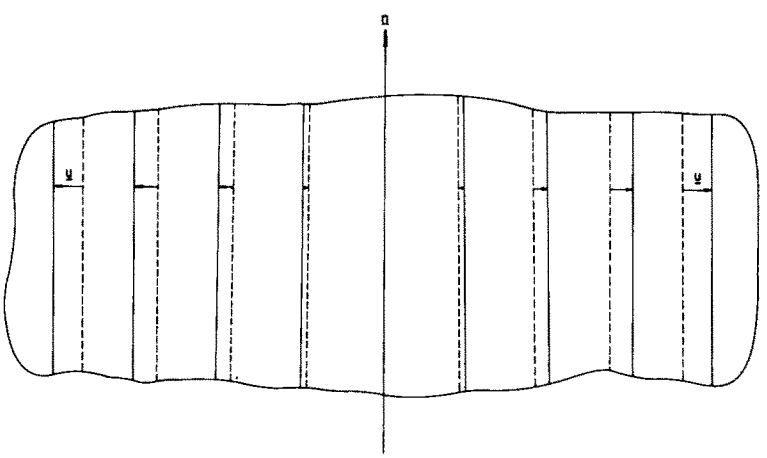

FIG. 5. Displacements corresponding to the N–C waves.

Setting (33) into (26) and employing (32) we obtain for the N–C wave:

$$u_1 = D[q_1 - (\mathbf{n} \cdot \mathbf{q})n_1] \tag{34.1}$$

$$u_2 = D[-(\mathbf{n} \cdot \mathbf{q})n_2] \tag{34.2}$$

$$u_3 = D[q_3 - (\mathbf{n} \cdot \mathbf{q})n_3] \tag{34.3}$$

$$\sigma_{31} = \bar{D}[(1+n_2^2)q_1 q_3 - n_1 n_3] \tag{34.4}$$

$$\sigma_{32} = \bar{D}[(q_1^2 - 1)n_2 n_3 - q_1 q_3 n_1 n_2] \tag{34.5}$$

$$\sigma_{33} = \bar{D}[1 - n_3^2 - (1+n_2^2)q_1^2]. \tag{34.6}$$

In (34) $D = A/|\mathbf{n} \times \mathbf{q}|\, e^{i\omega(\mathbf{s}\cdot\mathbf{x}-t)}$ and $\bar{D} = i\omega(\mu/c_2)D$. It was again assumed that $q_2 = 0$, while q_3 is related to q_1 by (42) as shown later.

2. *Consider* $\mathbf{s} \cdot \mathbf{n} = 0$

In this case the equations of motion (18) read

$$[(\lambda+\mu)s_j s_k + (\mu s^2 - \rho)\delta_{jk}]p_k = 0. \tag{35}$$

The determinant of (35) yields

$$(\mu s^2 - \rho)^2[(\lambda+2\mu)s^2 - \rho] = 0.$$

(i) Assume $\mu s^2 - \rho = 0$. In this case (35) yields $\mathbf{s} \cdot \mathbf{p} = 0$.

Since $\mathbf{p} \perp \mathbf{n}$ was already considered in equation (28), the linearly independent displacement which satisfies $\mathbf{q} \cdot \mathbf{p} = 0$ at the equator of the sphere is

$$\mathbf{p} = \mathbf{n}. \tag{36}$$

This displacement is associated with shear in the direction of fibers. The resulting wave will be denoted as the N–S wave (Fig. 6).

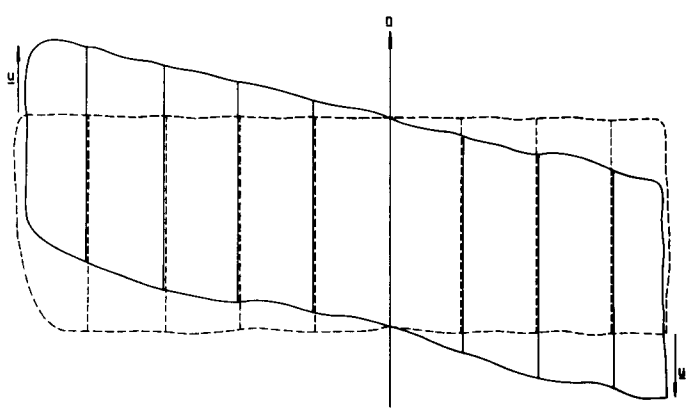

FIG. 6. Displacements corresponding to the N–S waves.

For the N–S wave we get:

$$u_1 = Ln_1 \tag{37.1}$$

$$u_2 = Ln_2 \tag{37.2}$$

$$u_3 = Ln_3 \tag{37.3}$$

$$\sigma_{31} = \bar{L}(n_3 q_1 + n_1 q_3) \tag{37.4}$$

$$\sigma_{32} = \bar{L} n_2 q_3 \tag{37.5}$$

$$\sigma_{33} = 2\bar{L} n_3 q_3 . \tag{37.6}$$

In (37) $L = A\, e^{i\omega(\mathbf{s}.\mathbf{x}-t)}$, $\bar{L} = i\omega(\mu/c_2)L$.

(ii) Assume $(\lambda+2\mu)s^2 - \rho = 0$.

This case turns out to be a part of the case $\mathbf{p} \cdot \mathbf{n} = 0$ already covered by equation (31).

3. *An exceptional case*

It can be observed that expressions (28), (30), (32) and (34) become indeterminate when $\mathbf{q} = \mathbf{n}$, namely when the slowness vector is parallel to the fiber direction. This case corresponds to the points at the poles in Fig. 3.

Since it has been assumed, without loss of generality, that $q_2 = 0$, the condition $\mathbf{q} = \mathbf{n}$ yields $\mathbf{n} = n_1\mathbf{e}_1 + n_3\mathbf{e}_3$.

It is easy to see that when $n_2 = 0$ we obtain:

(i) For the T–S wave:

$$\mathbf{p} = \mathbf{e}_2$$

so that

$$\begin{aligned} u_1 &= 0 \\ u_2 &= A\, e^{i\omega(\mathbf{s}.\mathbf{x}-t)} \\ u_3 &= 0 \\ \sigma_{31} &= 0 \\ \sigma_{32} &= Ai\omega(\mu/c_2)\, e^{i\omega(\mathbf{s}.\mathbf{x}-t)} q_3 \\ \sigma_{33} &= 0. \end{aligned} \tag{38}$$

(ii) For the $N-C$ wave. Here also $\mathbf{p} \cdot \mathbf{n} = 0$, therefore

$$\begin{aligned} u_1 &= -Bn_3 \\ u_2 &= 0 \\ u_3 &= Bn_1 \\ \sigma_{31} &= \bar{B}(n_1 q_1 - n_3 q_3) = \bar{B}(n_1^2 - n_3^2) \\ \sigma_{32} &= 0 \\ \sigma_{33} &= 2\bar{B} n_1 q_3 = 2\bar{B} n_1 n_3 . \end{aligned} \tag{39}$$

In (39) $B = A\,e^{i\omega(\mathbf{s}.\mathbf{x}-t)}$ and $\bar{B} = i\omega(\mu/c_2)B$.

4. *Arbitrary reaction*

Consider $\mathbf{s}\,.\,\mathbf{n} = 0$ and $\tau = i\omega T_0\,e^{i\omega(\mathbf{s}.\mathbf{x}-t)}$ and assume that the displacement field $\mathbf{u}$ vanishes identically.

In this case the stress field is given by

$$\sigma_{ij} = n_i n_j \tau = n_i n_j T_0 i\omega\,e^{i\omega(\mathbf{s}.\mathbf{x}-t)}.$$

The equations of motion reduce now to

$$\sigma_{ij,j} = n_i n_j s_j T_0(-\omega^2)\,e^{i\omega(\mathbf{s}.\mathbf{x}-t)} = 0.$$

Therefore, in the case of rigid fibers, it is possible to have a motionless, self-equilibrating traction field.

The existence of this field compensates for the absence of a third slowness surface in the case of rigid fibers. The condition $\mathbf{s}\,.\,\mathbf{n} = 0$ indicates that the arbitrary traction field is the trace of the flattened-out portions of the slowness surfaces in Fig. 2.

The traction, across any surface $x_3 = \text{const.}$, due to the arbitrary reaction field (A–R) is given by:

$$\begin{aligned}\sigma_{31} &= T_0 n_3 n_1 i\omega\,e^{i\omega(\mathbf{s}.\mathbf{x}-t)}\\ \sigma_{32} &= T_0 n_3 n_2 i\omega\,e^{i\omega(\mathbf{s}.\mathbf{x}-t)}\\ \sigma_{33} &= T_0 n_3^2 i\omega\,e^{i\omega(\mathbf{s}.\mathbf{x}-t)}.\end{aligned} \tag{40}$$

Also $u_1 = u_2 = u_3 = 0$.

When the plane $\mathbf{q}\,.\,\mathbf{n} = 0$ intersects the sphere $|\mathbf{q}| = 1$ along the equator the motionless arbitrary traction field no longer exists and must be replaced by the N–S wave. This case occurs when $q_3 = -(n_1/n_3)q_1 = \pm\sqrt{(1-q_1^2)}$.

GROUP VELOCITIES AND ENERGY FLUXES

The following was shown to hold for the T–S wave:

$$\overset{TS}{q_3} = \pm\sqrt{(1-q_1^2)}. \tag{41}$$

Equation (25) yields for the N–C wave:

$$\overset{NC}{q_3} = \frac{f_2(v)n_1 n_3 q_1 \pm F(v, q_1, \mathbf{n})}{1-f_2(v)n_3^2} \tag{42}$$

where

$$F(v, q_1, \mathbf{n}) = \{f_1(v)[1-f_2(v)n_3^2]-[1-f_2(v)(1-n_2^2)]q_1^2\}^{\frac{1}{2}} \tag{43}$$

and

$$f_1(v) = \frac{1-2v}{2(1-v)}, \qquad f_2(v) = \frac{1}{2(1-v)} = 1-f_1(v)$$

denote the dimensionless group velocity by $\mathbf{V}^g$. We have [6, 7]:

$$\mathbf{V}^g = \frac{\nabla D(\mathbf{q})}{\mathbf{q} \cdot \nabla D(\mathbf{q})}. \tag{44}$$

In (44) $D(\mathbf{q}) = 0$ is the expression for the slowness surface under consideration. The energy flux $\langle E_i \rangle$ is given by [6]:

$$\langle E_i \rangle = -\langle \operatorname{Re} \tau_{ij} \operatorname{Re} \dot{u}_j \rangle.$$

Employing (7) and (5) we obtain

$$\langle E_i \rangle = \tfrac{1}{2}(\omega^2/c_2)A\{[(\lambda+\mu)(\mathbf{q} \cdot \mathbf{p})p_i + \mu q_i]A + c_2\tau(\mathbf{n} \cdot \mathbf{p})n_i\}. \tag{45}$$

For each type wave equations (44) and (45) reduce further as follows:

1. *T–S wave*

For this wave $D(\mathbf{q}) = q_1^2 + q_3^2 - 1 = 0$. Therefore

$$\overset{TS}{V^g} = q_1\mathbf{e}_1 \pm \sqrt{(1-q_1^2)}\mathbf{e}_3. \tag{46}$$

Also, since $\mathbf{n} \cdot \mathbf{p} = 0$ and $\mathbf{q} \cdot \mathbf{p} = 0$ we have

$$\overset{TS}{\langle \mathbf{E} \rangle} = \tfrac{1}{2}\omega^2 A^2(\mu/c_2)(q_1\mathbf{e}_1 \pm \sqrt{(1-q_1^2)}\mathbf{e}_3). \tag{47}$$

In view of (46) it is clear that a positive sign has to be taken in (47) if the wave propagates in the positive x_3 direction and vice versa.

2. *N–C wave*

For this case equation (25) yields

$$(1-2\nu)D(\mathbf{q}) = 2(1-\nu)(q_1^2+q_3^2) - (q_1n_1 + q_3n_3)^2 - (1-2\nu) = 0.$$

Therefore,

$$\overset{NC}{\mathbf{V}^g} = \frac{1}{1-2\nu}\left\{[2(1-\nu)q_1 - \overset{NC}{(\mathbf{q} \cdot \mathbf{n})}n_1]\mathbf{e}_1 + [2(1-\nu)\overset{NC}{q_3} - \overset{NC}{(\mathbf{q} \cdot \mathbf{n})}n_3]\mathbf{e}_3\right\}. \tag{48}$$

In view of (44), we obtain

$$\overset{NC}{\mathbf{V}^g} = \frac{1}{1-2\nu}\left\{[2(1-\nu)q_1 - \overset{NC}{(\mathbf{q} \cdot \mathbf{n})}n_1]\mathbf{e}_1 \pm \overset{NC}{F(\nu, \mathbf{q}, \mathbf{n})}\mathbf{e}_3\right\}.$$

The quantity $F(\nu, \mathbf{q}, \mathbf{n})$ is given in (43).

Now, for $N-C$ wave $c_2\tau = -A(\lambda+\mu)\mathbf{q} \cdot \mathbf{p}$, whereby

$$\overset{NC}{\langle E_i \rangle} = \tfrac{1}{2}(\omega^2/c_2)A^2\{(\lambda+\mu)\ (\mathbf{q} \cdot \mathbf{p})[p_i - (\mathbf{n} \cdot \mathbf{p})n_i] + \mu q_i\}.$$

In general

$$p_i - (\mathbf{n} \cdot \mathbf{p})n_i = [(\mathbf{n} \times \mathbf{p}) \times \mathbf{n}]_i$$

but for the $N-C$ wave $\mathbf{p} \cdot \mathbf{n} = 0$ so that $(\mathbf{n} \times \mathbf{p}) \times \mathbf{n} = \mathbf{p}$ thus

$$\overset{NC}{\langle E_i \rangle} = \tfrac{1}{2}\omega^2 A^2(\mu/c_2)\left\{2\frac{1-\nu}{1-2\nu}q_i - \frac{1}{1-2\nu}(\mathbf{n} \cdot \mathbf{q})n_i\right\}. \tag{49}$$

In view of (48) it is clear that a positive sign has to be taken in (42) for waves propagating in the positive x_3 axis and vice versa.

3. *N–S wave*

In view of Fig. 2 it is clear that at the equator the group velocity $\overset{NS}{\mathbf{V}}_g = \overset{TS}{\mathbf{V}}_g$. Similarly, one can readily find that $\langle \overset{NC}{\mathbf{E}} \rangle = \langle \overset{TS}{\mathbf{E}} \rangle$. Therefore, equations (46), (47) are valid for the *N–S* wave also.

SURFACE WAVES

For the existence of surface waves, decaying away from the surface $x_3 = 0$, it is required that q_1 be real while $\overset{NC}{q}_3, \overset{TS}{q}_3$ be both complex or imaginary. This means that the more severe of the following conditions

$$q_1^2 > 1$$
$$q_1^2 > \frac{1-f_2(v)n_3^2}{1-f_2(v)(1-n_2^2)} f_1(v) = \frac{1-2v}{2(1-v)} \frac{2(1-v)-n_3^2}{2(1-v)-(n_1^2+n_3^2)} \tag{50}$$

must be satisfied.

In view of (50) we have:

For $n_3^2 < 2(1-v)(1-n_1^2)$ it is necessary and sufficient to have $q_1^2 > 1$.

For $n_3^2 > 2(1-v)(1-n_1^2)$ it is necessary and sufficient to have

$$q_1^2 > \frac{1-2v}{2(1-v)} \frac{2(1-v)-n_3^2}{2(1-v)-(n_1^2+n_3^2)}.$$

Employing equations (30), (34) and (40) the vanishing of the traction at $x_3 = 0$ requires

$$\begin{vmatrix} \overset{TS}{n_2(q_3^2-q_1^2)} & \overset{NC}{(1+n_2^2)q_1q_3-n_1n_3} & n_1 \\ \overset{TS\ TS}{(n_3q_1-n_1q_3)q_3} & \overset{NC}{(q_1^2-1)n_2n_3-q_1q_3n_1n_2} & n_2 \\ \overset{TS}{-2n_2q_1q_3} & 1-n_3^2-(1+n_2^2)q_1^2 & n_3 \end{vmatrix} = 0. \tag{51}$$

In view of (41) and (42), (51) becomes an equation for q_1. If q_1 satisfies the restrictions (50) then surface waves exist.

Rather than investigate the complete solution of (51), it suffices for the purpose of the present discussion to consider some special sub-cases.

Assume for instance that $n_1 = 0$. In this case the determinant (51) simplifies to

$$\left(\frac{n_2}{1+n_2^2}\right)^2 (1-2q_1^2)^2 = -q_1^2 \overset{TSNC}{q_3 q_3}. \tag{52}$$

The solution of (52) was obtained numerically with the aid of an electronic computer.

It has been shown that for $v = 0$ and $v = \frac{1}{4}$ there exists a real root $q_1 > 1$ for all values of $|n_2| \leq 1$. This means that surface waves are feasible. Values of q_1 vs. n_2 which solve (52) are plotted in Fig. 7.

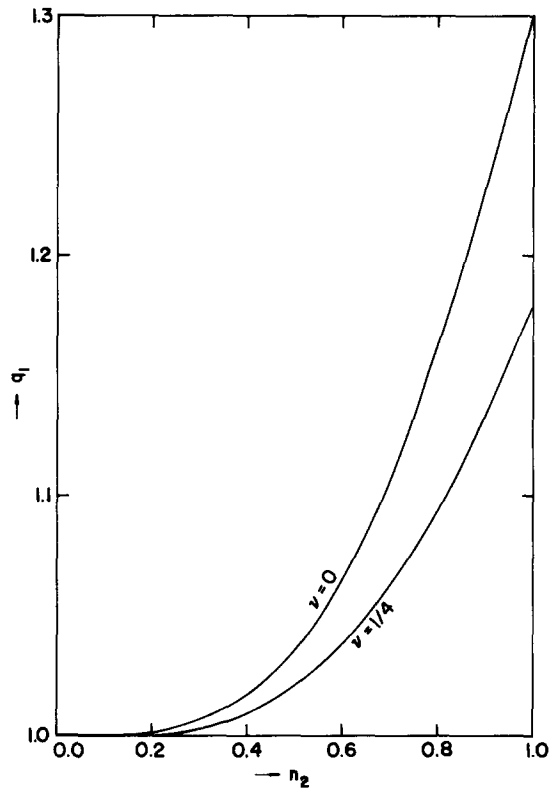

FIG. 7. Values of q_1 vs. n_2, which solve equation (52).

It may be noted that when $n_2 = 1$, namely when the fibers are perpendicular to the plane of wave propagation, the Rayleigh surface wave is reproduced.

REFLECTION AND REFRACTION OF PLANE HARMONIC WAVES

Consider two semi-infinite media, with common Lamé constants λ and μ, bonded to each other at the plane $x_3 = 0$. Let the directions of the fibers be $\mathbf{n}$ for $x_3 < 0$ and $\mathbf{N}$ for $x_3 > 0$.

Let an incident N–C or T–S wave, which propagates from the medium $\mathbf{n}$ toward the medium $\mathbf{N}$, impinge on the interface $x_3 = 0$. Due to the abrupt change in the direction of the fibers, every incident wave will decompose into reflected and refracted waves of all types.

For any given $\mathbf{n}$ and $\mathbf{N}$ consider an incident wave of the form

$$\overset{(I)}{\mathbf{u}} = \overset{(I)(I)}{A}\,\mathbf{p} \exp i\omega(\overset{(I)}{\mathbf{s}} \cdot \mathbf{x} - t). \tag{53}$$

The corresponding reflected waves are

$$\begin{aligned}
\overset{NC}{\mathbf{u}} &= \overset{NC\,NC}{A}\ \overset{NC}{\mathbf{p}} \exp i\omega(\overset{NC}{\mathbf{s}}\cdot\mathbf{x}-t)\\
\overset{TS}{\mathbf{u}} &= \overset{TS\,TS}{A}\ \overset{TS}{\mathbf{p}} \exp i\omega(\overset{TS}{\mathbf{s}}\cdot\mathbf{x}-t)\\
\overset{NS}{\mathbf{u}} &= \overset{NS\,NS}{A}\ \overset{NS}{\mathbf{p}} \exp i\omega(\overset{NS}{\mathbf{s}}\cdot\mathbf{x}-t).
\end{aligned} \tag{54}$$

In general, however, the last of (54) will be replaced by the following field of arbitrary tractions:

$$\overset{AR}{\sigma_{kj}} = \overset{AR}{A}\ n_k n_j \exp i\omega\ (\overset{AR}{\mathbf{s}}\cdot\mathbf{x}-t). \tag{55}$$

In view of (28), (32) and (36) the quantities $\overset{NC}{\mathbf{p}}$, $\overset{TS}{\mathbf{p}}$ and $\overset{NS}{\mathbf{p}}$ can be expressed in terms of $\mathbf{n}$ and the respective slowness $\mathbf{q}$.

Similarly, the refracted waves are given by:

$$\begin{aligned}
\overset{NC}{\mathbf{u}'} &= \overset{NC\,NC}{A'}\ \overset{NC}{\mathbf{p}'} \exp i\omega(\overset{NC}{\mathbf{s}'}\cdot\mathbf{x}-t)\\
\overset{TS}{\mathbf{u}'} &= \overset{TS\,TS}{A'}\ \overset{TS}{\mathbf{p}'} \exp i\omega(\overset{TS}{\mathbf{s}'}\cdot\mathbf{x}-t)\\
\overset{NS}{\mathbf{u}'} &= \overset{NS\,NS}{A'}\ \overset{NS}{\mathbf{p}'} \exp i\omega(\overset{NS}{\mathbf{s}'}\cdot\mathbf{x}-t).
\end{aligned} \tag{56}$$

The refracted N–S wave is excited only when $\overset{NS}{q_3} = -(N_1/N_3)\overset{NS}{q_1} = \pm\sqrt{(1-\overset{NS}{q_1^2})}$, otherwise, the last of (56) is replaced by the field of arbitrary tractions as follows:

$$\overset{AR}{\sigma'_{kj}} = \overset{AR}{A'}N_k N_j \exp i\omega(\overset{AR}{\mathbf{s}'}\cdot\mathbf{x}-t). \tag{57}$$

In (56) the quantities $\mathbf{p}'$ can be expressed in terms of $\mathbf{N}$ and the relevant $\mathbf{q}'$ by means of (28), (32) and (36).

The condition of perfect bonding at $x_3 = 0$ requires continuity of tractions and displacements at all points on the interface and for all time. Therefore $q'_1x'_1+q'_2x_2 = \overset{I}{q_1}x_1+\overset{I}{q_2}x_2 = q_1x_1+q_2x_2$ for all x_1 and x_2. Thus: $q'_1 = q_1 = \overset{I}{q_1}$ for all wave forms. In addition, since we take (without loss of generality) $\overset{I}{q_2} = 0$ it follows that $q_2 = q'_2 = 0$ for all wave forms.

Furthermore, in view of (41) and (42) we have

$$\overset{TS}{q'_3} = -\overset{TS}{q_3} = \sqrt{(1-q_1^2)}$$

$$\overset{NC}{q_3} = \frac{f_2n_1n_3q_1-F(v,q_1,\mathbf{n})}{1-f_2n_3^2}, \qquad \overset{NC}{q_3'} = \frac{f_2N_1N_3q_1+F(v,q_1,\mathbf{N})}{1-f_2N_3^2}$$

so that the various vectors $\mathbf{p}$ can in fact be related to $\mathbf{n}$ and q_1, or to $\mathbf{N}$ and q_1, only.

Altogether there exist six unknown amplitudes in the diffraction problem. These unknowns are the amplitudes $\overset{TS}{A}, \overset{NC}{A}, \overset{AR}{A}, \overset{TS}{A'}, \overset{NC}{A'}$ and $\overset{AR}{A'}$. Under exceptional circumstances $\overset{AR}{A}$ is replaced by $\overset{NS}{A}$ or $\overset{AR}{A'}$ is replaced by $\overset{NS}{A'}$.

These six unknowns are determined from the six boundary conditions at $x_3 = 0$ which require that

$$u_i(x_1, x_2, 0, t) = u_i'(x_1, x_2, 0, t)$$

and

$$\sigma_{3i}(x_1, x_2, 0, t) = \sigma_{3i}'(x_1, x_2, 0, t).$$

The six by six system of equations is tabulated below:

$\overset{TS}{A}$ $\overline{\lvert\mathbf{n}\times\mathbf{q}\rvert}$	$\overset{NC}{A}$ $\overline{\lvert\mathbf{n}\times\mathbf{q}\rvert}$	$\overset{AR}{-A}$	$\overset{TS}{A'}$ $\lvert\mathbf{N}\times\mathbf{q}\rvert$	$\overset{NC}{A'}$ $\lvert\mathbf{N}\times\mathbf{q}\rvert$	$\overset{AR}{A'}$	$\overset{(I)}{A}$
$\overset{TS}{n_2 q_3}$	$\overset{NC}{q_1}-(\mathbf{n}\cdot\mathbf{q})n_1$	0	$\overset{TS}{N_2 q_3'}$	$\overset{NC}{q_1}-(\mathbf{N}\cdot\mathbf{q}')N_1$	0	$\overset{(I)}{a_1}$
$\overset{TS}{n_3 q_1}-n_1 q_3$	$\overset{NC}{-(\mathbf{n}\cdot\mathbf{q})n_2}$	0	$\overset{TS}{N_3 q_1}-N_1 q_3'$	$\overset{NC}{-(\mathbf{N}\cdot\mathbf{q}')N_2}$	0	$\overset{(I)}{a_2}$
$-n_2 q_1$	$\overset{NC}{q_3}-\overset{NC}{(\mathbf{n}\cdot\mathbf{q})}n_3$	0	$-N_2 q_1$	$\overset{NC}{q_3'}-\overset{NC}{(\mathbf{N}\cdot\mathbf{q}')}N_3$	0	$\overset{(I)}{a_3}$
$\overset{TS}{n_2}(q_3^2-q_1^2)$	$\overset{NC}{(1+n_2^2)}q_1 q_3-n_1 n_3$	n_1	$\overset{TS}{N_2}(q_3'^2-q_1^2)$	$\overset{NC}{(1+N_2^2)}q_1 q_3'-N_1 N_3$	N_1	$\overset{(I)}{a_4}$
$\overset{TS\ TS}{(n_3 q_1}-n_1 q_3)q_3$	$\overset{NC}{(q_1^2-1)}n_2 n_3-q_1 q_3 n_1 n_2$	n_2	$\overset{TS\ TS}{(N_3 q_1}-N_1 q_3')q_3'$	$\overset{NC}{(q_1^2-1)}N_2 N_3-q_1 q_3' N_1 N_2$	N_2	$\overset{(I)}{a_5}$
$\overset{TS}{-2n_2 q_1 q_3}$	$1-n_3^2-(1+n_2^2)q_1^2$	n_3	$\overset{TS}{-2N_2 q_1 q_3'}$	$1-N_3^2-(1+N_2^2)q_1^2$	N_3	$\overset{(I)}{a_6}$

(58)

The first three equations are obtained from continuity of displacements and the last three equations are derived from continuity of tractions.

In (58) the column $\overset{(I)}{A}$ represents quantities related to the incident wave. For an incident $T-S$ wave the entries $\overset{(I)}{a_1}$–$\overset{(I)}{a_6}$ are obtained from (30). For an incident $N-C$ wave those entries are obtained from (34). In the present work the amplitude of each incident wave was "normalized" so that it always corresponds to $\langle \overset{(I)}{E_3} \rangle = 1$.

This normalization provides a direct indication of the relative portions of energy that are carried by the reflected and the refracted waves.

In the particular case $q_1 = n_3/(n_1^2+n_3^2)^{\frac{1}{2}}$ the column $\overset{AR}{-A}$ must be replaced by a column based upon (37), with $\overset{NS}{q_3} = -\sqrt{1-q_1^2}$. Analogously, when $q_1 = -N_3/(N_1^2+N_3^2)^{\frac{1}{2}}$ a refracted N–S wave is excited and the column $\overset{AR}{A'}$ must be replaced by a column like (37), with $\mathbf{n} \to \mathbf{N}$. In this case $\overset{NS}{q_3'} = \sqrt{(1-q_1^2)}$.

The refracted fluxes of energy $\overset{NC}{E_3'}, \overset{TS}{E_3'}, \overset{NS}{E_3'}$ and the reflected energy fluxes $\overset{NC}{E_3}, \overset{TS}{E_3}, \overset{NS}{E_3}$ are evaluated according to equations (47) and (49).

A check on the results is provided by the requirement of balance of energy flux:

$$\overset{(I)}{E_3}+\overset{NC}{E_3}+\overset{TS}{E_3}+\overset{NS}{E_3}=\overset{NC}{E'_3}+\overset{TS}{E'_3}+\overset{NS}{E'_3}. \tag{59}$$

This check was performed for all results presented herein.

Finally it should be recalled that for complex values of q_3 (evanescent waves) the energy flux is directed parallel to the interface $x_3 = 0$, so that $E_3 = 0$ [10]. In the present work criteria for evanescence are given in (50).

Furthermore, since all incident waves are assumed to be propagating, it follows from (41)–(43) that for incident T–S waves $|q_1| < 1$ while for incident N–C waves

$$|q_1| < \left[\frac{f_1(1-f_2n_3^2)}{1-f_2(1-n_2^2)}\right]^2.$$

A representative solution for diffraction of plane harmonic waves is exhibited in Figs. 8 and 9. All computations were performed on an electronic computer. Specific values of **n** and **N** were taken as follows:

$$n_1 = 0{\cdot}2, \quad n_2 = 0{\cdot}5, \quad n_3 = \sqrt{0{\cdot}71}; \qquad N_1 = 0{\cdot}4, \quad N_2 = 0{\cdot}7, \quad N_3 = \sqrt{0{\cdot}35}.$$

The value of Poisson's ratio was taken to be $\nu = 0$. In each computation the amplitude of the incident wave was normalized to give $E_3 = 1$. The results for an incident T–S wave are plotted v. q_1 in Fig. 8, with $-1 < q_1 < 1$. Note that, in general, only two reflected and two refracted energies are involved, since the energy-less arbitrary reactions are activated in most cases.

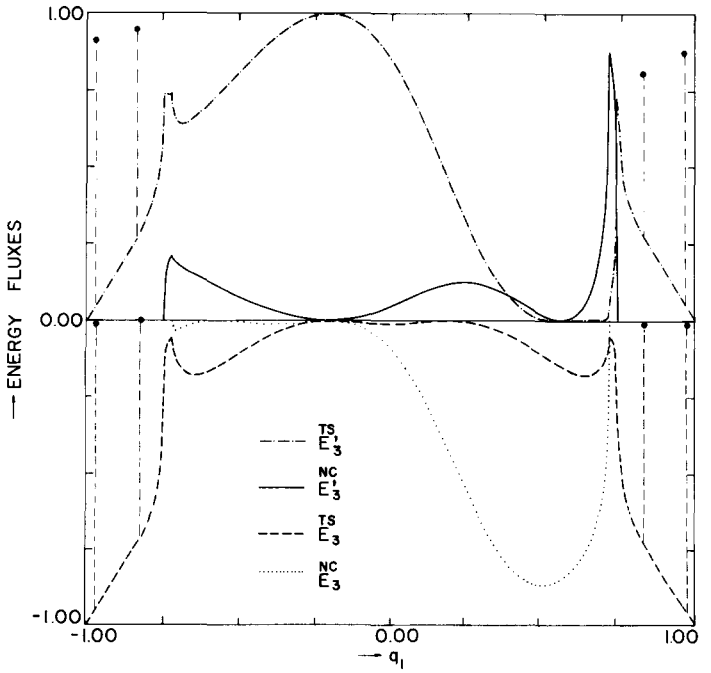

FIG. 8. Reflected and refracted energy fluxes corresponding to an incident T–S wave vs. q_1.

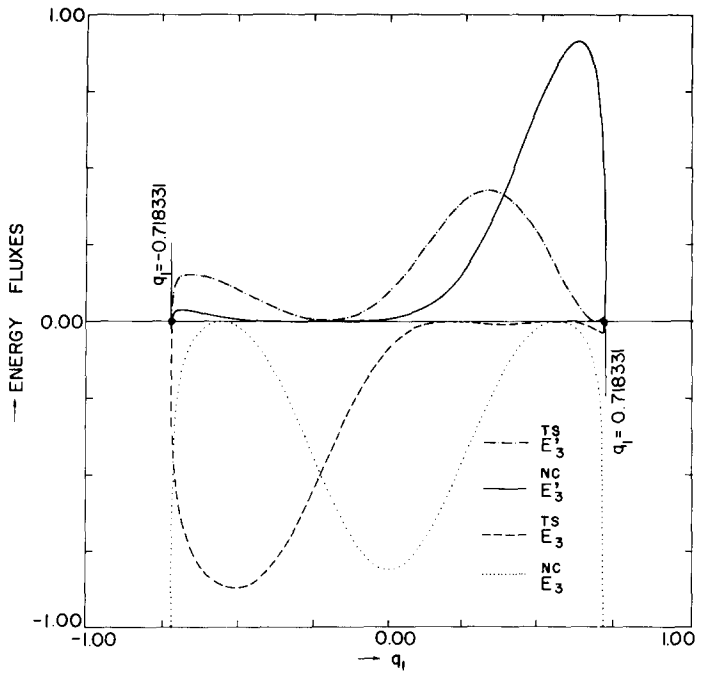

FIG. 9. Reflected and refracted energy fluxes corresponding to an incident N–C wave vs. q_1.

Exceptions occur when $q_1 = \pm n_3/(n_1^2+n_3^2)^{\frac{1}{2}} = \pm 0{\cdot}972968$ and at $q_1 = \pm N_3/(N_1^2+N_3^2)^{\frac{1}{2}} = \pm 0{\cdot}828417$. In those cases, reflected or refracted N–S waves are excited and their participation in the differcation phenomenon gives rise to points of discontinuity in Fig. 8.†

In these cases the entries at third, or the sixth, column in (58) should be appropriately selected according to (37). The details are presented more elaborately in equations (60) through (68). The numerical results at these values of q_1 are:

TABLE 1

q_1	E_3^{TS}	E_3^{NC}	E_3^{NS}	$E_3'^{TS}$	$E_3'^{NC}$	$E_3'^{NS}$
−0·972968	−0·009298	0	−0·069856	0·920846	0	0
−0·828417	0	0	0	0·951349	0	0·048651
+0·828417	0	0	0	0·862164	0	0·137836
+0·972968	−0·009298	0	−0·108173	0·882528	0	0

Note that the reflected and refracted N–C waves become evanescent for $|q_1| > 0{\cdot}718331$ and $|q_1| > 0{\cdot}744104$, respectively.

† The presence of "atoms" is directly attributable to the assumption of fiber inextensibility. Due to the inextensibility, N–S waves are excited only in singular directions (the directions normal to the fibers). It will be shown in a forthcoming paper that when the fibers are even slightly extensible the "atoms" no longer exist and all curves are continuous.

The results for an incident N–C wave are exhibited in Fig. 9. In this case q_1 covers the range $-0{\cdot}718331 < q_1 < 0{\cdot}718331$, where a propagating N–C wave exists. In the present range no N–S waves are excited.

It is worth noting that the curve in Fig. 8, which gives the energy flux of the reflected N–C wave due to an incident T–S wave, is a mirror image in q_1 of the curve drawn in Fig. 9, which represents the energy flux of the reflected T–S wave due to an incident N–C wave.

REFRACTION OF INCIDENT N–S WAVES

It is impossible to analyze the case of incident N–S waves by means of expressions derived for rigid fibers. The reason for the difficulty is that no distinction can be made between the slowness vectors of the incident and reflected N–S waves, because for the rigid fibers those two vectors must lie on the equator of the slowness sphere $|\mathbf{q}| = 1$.

In order to overcome the difficulty we employ equations (16) and (17) for large γ and small values of $\cos\theta$. For small $\cos\theta$ these equations yield

$$c^2(q_1n_1+q_3n_3)^2+q_1^2+q_3^2 = 1, \qquad \mathbf{p} = \mathbf{n}. \tag{60}$$

In (60) the notation $\mathbf{q} = c_2\mathbf{s}$ and $\gamma/\mu = c^2$ was employed.

Solving the first of (60) for q_3 we get

$$q_3^{\pm} = \frac{-c^2n_1n_3q_1 \pm \sqrt{\{1+c^2n_3^2-[c^2(n_1^2+n_3^2)+1]q_1^2\}}}{1+c^2n_3^2}. \tag{61}$$

However, since the slowness vector of the incident wave lies on the equator we have $q_1 = -n_3/\sqrt{(n_1^2+n_3^2)}$, as may be deduced from Fig. 2. Therefore, we obtain from (61)

$$q_3^+ = \frac{n_1}{\sqrt{(n_1^2+n_3^2)}}, q_3^- = \frac{c^2n_3^2-1}{c^2n_3^2+1}\frac{n_1}{\sqrt{(n_1^2+n_3^2)}}. \tag{62}$$

Furthermore, we get

$$\mathbf{n}\cdot\mathbf{q}^+ = 0 \tag{63}$$

and, as $c^2 \to \infty$,

$$\mathbf{n}\cdot\mathbf{q}^- = -2\frac{n_1n_3}{\sqrt{(n_1^2+n_3^2)}}\frac{1}{c^2n_3^2}. \tag{64}$$

After straightforward calculations, we obtain the following values for the component of the group velocity in the x_3 direction:

$$V_3^g(q_3^+) = \frac{n_1}{\sqrt{(n_1^2+n_3^2)}}$$

$$V_3^g(q_3^-) = -\frac{n_1}{\sqrt{(n_1^2+n_3^2)}}.$$

Hence, the slowness vector $\mathbf{q}^+ = q_1\mathbf{e}_1+q_3^+\mathbf{e}_3$ is associated with a wave impinging on the interface, while the slowness vector $\mathbf{q}^- = q_1\mathbf{e}_1+q_3^-\mathbf{e}_3$ is related to a reflected wave.

Furthermore, in view of (6) and the $(60)_2$, we obtain the following expressions for displacements and stresses:

$$u_i = Bp_i, \qquad \sigma_{ij} = \bar{B}\left[\frac{2\nu}{1-2\nu}n_k q_k \delta_{ij} + n_i q_j + n_j q_i + c^2 n_k q_k n_i n_j\right]. \tag{65}$$

In (65) $B = e^{i\omega(\mathbf{s}.\mathbf{x}-t)}$ and $\bar{B} = (i\omega\mu/c_2)B$. The expression for the energy flux becomes

$$\langle E_i \rangle = \tfrac{1}{2}\omega^2 A^2(\mu/c_2)\left[\left(\frac{1}{1-2\nu}+c^2\right)(\mathbf{n}.\mathbf{q})n_i + q_i\right]. \tag{66}$$

Setting (62) and (64) into (65) and (66), then taking the limit as $c^2 \to \infty$ we get the following.

1. *For the incident N–S wave*

$$\begin{gathered} u_1 = n_1, \qquad u_2 = n_2, \qquad u_3 = n_3, \\ \sigma_{31} = (n_1^2 - n_3^2)(n_1^2+n_3^2)^{-\frac{1}{2}}, \qquad \sigma_{32} = n_1 n_2 (n_1^2+n_3^2)^{-\frac{1}{2}}, \qquad \sigma_{33} = 2n_1 n_3 (n_1^2+n_3^2)^{-\frac{1}{2}} \end{gathered} \tag{67}$$

and

$$\langle E_3 \rangle = n_1(n_1^2+n_3^2)^{-\frac{1}{2}}.$$

2. *For the reflected N–S wave*

$$\begin{gathered} u_1 = n_1, \qquad u_2 = n_2, \qquad u_3 = n_3, \\ \sigma_{31} = -(n_1^2+n_3^2)^{\frac{1}{2}}, \qquad \sigma_{32} = -n_1 n_2 (n_1^2+n_3^2)^{-\frac{1}{2}}, \qquad \sigma_{33} = 0 \end{gathered} \tag{68}$$

and

$$\overset{NS}{E}_3 = -A^2 n_1 (n_1^2+n_3^2)^{-\frac{1}{2}}.$$

The solution for the case of an incident N–S wave is obtained from equations (58). The entries for the incident column, $\overset{(I)}{a}_1$–$\overset{(I)}{a}_6$, are given in (67) and the column $-AR$ must be replaced by the entries listed in (68).

Employing the same values as before for the fiber directions $\mathbf{n}$ and $\mathbf{N}$ and for Poisson's ratio ν, we obtained the following numerical values for the refracted energies: at $q_1 = -n_3/\sqrt{(n_1^2+n_3^2)}$:

$$\overset{NS}{E}{}_3^{(I)} = 1{\cdot}0, \quad \overset{TS}{E}_3 = -0{\cdot}10817, \quad \overset{NC}{E}_3 = 0, \quad \overset{NS}{E}_3 = -0{\cdot}81267, \quad \overset{TS}{E}{}'_3 = 0{\cdot}07916, \quad \overset{NC}{E}{}'_3 = 0.$$

Entirely analogous results can be obtained at $q_1 = +n_3/(n_1^2+n_3^2)^{\frac{1}{2}}$, where incident and reflected N–S waves also occur simultaneously. In this case it can be shown that expressions (67) and (68) are still valid, except that the signs in front of the stresses must be reversed and the roles of incident waves and reflected waves must be interchanged.

SPECIAL CASES OF REFRACTION

1. *Consider* $n_2 = N_2 = 0$

In this case the slowness vector $\mathbf{q} = q_1\mathbf{e}_1 + q_3\mathbf{e}_3$ lies in the plane of $\mathbf{n}$ and $\mathbf{N}$. The following conclusions can be reached from inspection of equations (30), (34), (40) and (58).

In the case of an incident T–S wave the column $\overset{TS}{A'}$ becomes identical with the column $\overset{(I)}{A}$ in (58) regardless of the values of n_1, n_3, N_1 and N_3. Therefore the incident T–S wave proceeds undisturbed across the interface.

In the case of an incident N–C wave it can be observed, after some straightforward manipulations, that this wave will be entirely reflected as an N–C wave. This means that the interface will act as a perfect barrier against N–C waves.

This last conclusion, concerning N–C waves, is not valid under the exceptional conditions which enable the excitement of N–S waves.

2. *The case* $n_2 = 0, N_2 = \varepsilon \ll 1$

In this case it can be shown that the interface $x_3 = 0$ acts as a perfect barrier against incident T–S waves while it transmits N–C waves entirely. These conclusions are not valid under the exceptional circumstances when N–S waves are excited.

One should be cautioned that the conclusions for $n_2 = 0$ and $N_2 = \varepsilon$ are based on considerations of order of magnitude, with $\varepsilon \ll 1$. It is suspected that these conclusions may be restricted to rigid fibers only and are not valid for any finite values of γ, no matter how large.

CONCLUSIONS

In this paper it has been shown that in materials reinforced by straight, parallel and rigid fibers, there exist three types of harmonic, elastic waves. Two types of waves can propagate in any direction. One of these two waves is a compression-like wave with displacements perpendicular to the fibers. This wave is named the "normal compression" wave and denoted N–C. The second of the two waves is a shear wave with displacements in directions transverse to the fibers. This wave is named the "transverse shear" wave and denoted by T–S.

The third wave can propagate only in directions that are normal to the fibers. This wave corresponds to shearing deformation with displacements that are parallel to the direction of the fibers. In this case the motion is such that the fibers remain straight at all times. This wave is called the "normal shear" wave and denoted by N–S. The motions associated with the three waves were sketched in Figs. 4–6. In this paper, particular attention was paid to the dependence of the various wave characteristics on the direction of the fibers. It has been shown that if the same kinks are given to all fibers across a certain plane within the composite material, then this plane acts as a diffracting interface.

When an incident N–C, T–S or N–S wave impinges on such an interface it decomposes, in general, into all possible types of reflected and refracted waves. Attenuation occurs for incidence beyond some critical angles.

The reflected and refracted fluxes of energy for all three types of incident waves were analyzed in general and evaluated quantitatively for a specific example. In the example certain values were selected for the directions of the fibers on each side of the interface, so that the reflected and refracted energy fluxes remained dependent only on the direction of propagation. The dependence of the various energies on the direction of propagation was obtained with the aid of an electronic computer and was exhibited in Figs. 8 and 9.

These figures demonstrate the crucial effects that misalignments in fiber directions may have on the transmission of mechanical energy in fiber-reinforced composites. There

exist combinations of fiber directions and propagation directions which may hinder substantially the forward progress of energy. Such combinations may be employed advisedly to construct a desired filtering system or a wave guiding mechanism.

The practical significance of this work is limited by the range of applicability of the mathematical model employed herein. It has been indicated that the results are meaningful for a composite reinforced by very rigid fibers when the volume ratio of the fibers is small, when the length of the waves is large in comparison with the intra-fiber distances and when the Poisson ratio of the matrix material is close to zero. In order to gain better insight into the effects of fiber misalignments on the dynamic response of composites it may be worthwhile to remove the assumption of rigidity of the fibers. Such studies are being conducted currently and will be reported in the near future.†

Acknowledgements—The author wishes to express his indebtedness to Professor A. C. Pipkin of Brown University and to Dr. S. Frankenthal of Tel-Aviv University for many helpful discussions. The assistance of Mrs. D. Neulander and of Dr. J. Aboudi, of Tel-Aviv University, in obtaining the numerical results presented in this work, is gratefully acknowledged. This work was performed under contract DAJA-37-71-C-1579 of the U.S. Army. The author wishes to express his sincere thanks for this financial support.

REFERENCES

[1] Z. HASHIN, *Theory of Mechanical Behavior of Heterogeneous Media, Applied Mechanics Surveys*, pp. 263–275. Spartan (1966).
[2] Z. HASHIN, Theory of Fiber Reinforced Materials, Contract NAS 1-8818, NASA Langley Research Center (1970).
[3] G. W. POSTMA, Wave propagation in a stratified medium. *Geophysics* **20**, 780–805 (1955).
[4] S. M. RYTOV, Acoustical properties of a thinly laminated medium. *Soviet Phys. Acoust.* **2**, 68–80 (1956).
[5] J. ABOUDI and Y. WEITSMAN, Impact-deflection by oblique fibers in sparsely reinforced composites, to be published.
[6] M. J. P. MUSGRAVE, Elastic Waves in Anisotropic Media, *Progress in Solid Mechanics*, edited by I. N. SNEDDON and R. HILL, Vol. II, pp. 63–85. North Holland (1961).
[7] J. L. SYNGE, Elastic waves in anisotropic media. *J. Math. Phys.* **35**, 323–334 (1957).
[8] A. E. GREEN and J. E. ADKINS, *Large Elastic Deformations and Non-Linear Continuum Mechanics*, pp. 32–35, 216–258. Oxford University Press (1960).
[9] W. JAUNZEMIS, *Continuum Mechanics*, p. 307, equation (14.47). MacMillan (1967).
[10] J. L. SYNGE, Flux of Energy for Elastic Waves in Anisotropic Media. *Proc. R. Ir. Acad.* **A58**, 13–21 (1956).

(*Received* 1 *March* 1971; *revised* 4 *October* 1971)

Абстракт—Работа касается распространения упругих волн в материалах, усиленных нерастяжимыми волокнами. Определяются поверхности медленности, потоки энергии и направления распространения и эти зависимости представляются в выражениях свойств материалов и направлениях волокон.

Рассматривается, подробно, случай двух областей материалов, усиленных волокнами, похожими во всех отношениях, кроме направления волокна и соединенных с собой вдолв плоскости раздела. Указывается, что неправильные расположения по направлению волокон, встречающиеся вдоль плоскости соединения, вызывают значительное рассеяния механической энергии.

Приводится диапазон важности математической моделм, используемой в работе и указывается, что результаты могут быть использованы в практических случаях.

Обсуждается, также, вопрос существования поверхностных волн.

† Correction upon receiving proofs: upon further investigation it can be shown that the mathematical model employed herein is valid for any value of Poisson's ratio of the matrix material. Therefore restriction (4) on p. 629 can be removed without loss of generality. The details will be given in Ref. [5].